

PAPER

Lipidomic analysis reveals disturbances in glycerophospholipid and sphingolipid metabolic pathways in benzene-exposed mice

Linling Yu,^{1,†} Rongli Sun,^{1,†} Kai Xu,¹ Yunqiu Pu,¹ Jiawei Huang,¹ Manman Liu,¹ Minjian Chen,^{2,3} Juan Zhang,¹ Lihong Yin¹ and Yuepu Pu^{1,*}

¹Key Laboratory of Environmental Medicine Engineering, Ministry of Education, School of Public Health, Southeast University, Nanjing 210009, Jiangsu, China, ²State Key Laboratory of Reproductive Medicine, Institute of Toxicology, Nanjing Medical University, Nanjing 211166, China and ³Key Laboratory of Modern Toxicology of Ministry of Education, School of Public Health, Nanjing Medical University, Nanjing 211166, China

*Correspondence address. Professor Yuepu Pu, School of Public Health, Southeast University, 87 Dingjiaqiao Street, Nanjing 210009, P. R. China.

Tel: +86-25-83272582; Fax: +86-25-83272582; E-mail: yppu@seu.edu.cn

[†]These authors contributed equally to this work.

[†]These authors contributed equally to this work.

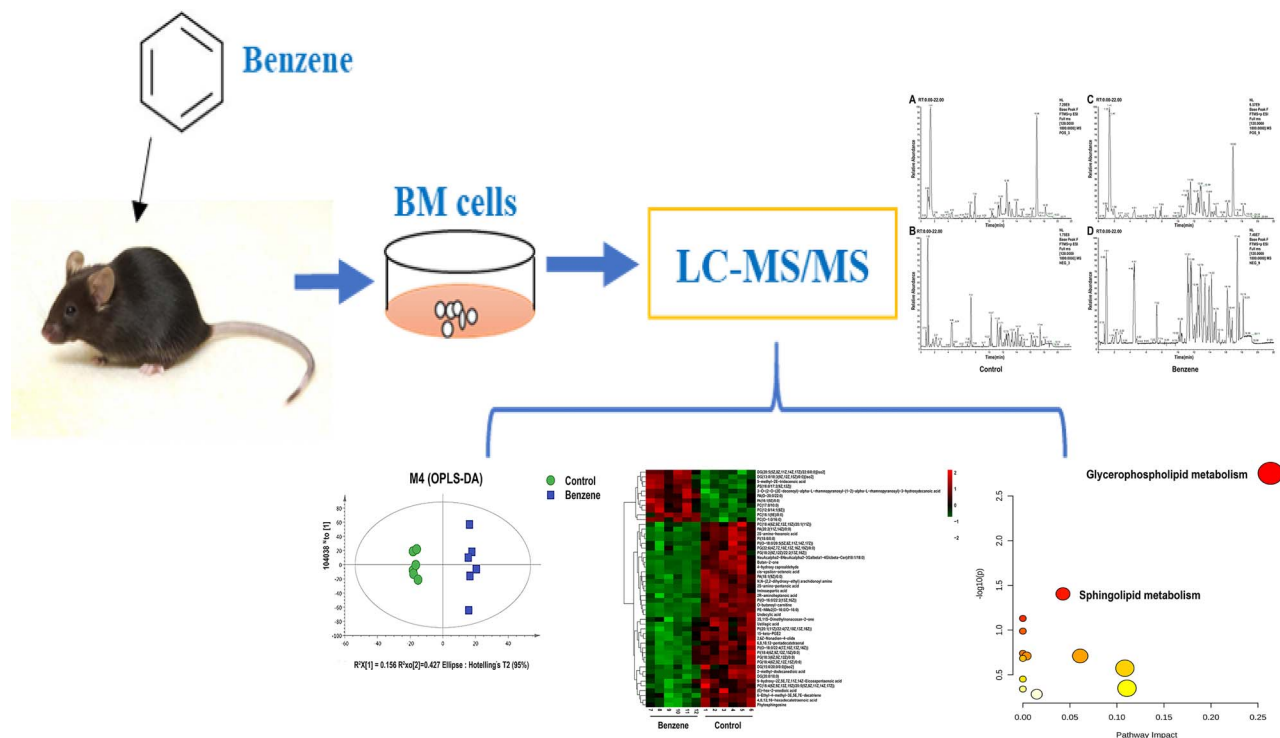
Abstract

Benzene, a known occupational and environmental contaminant, has been recognized as the hematotoxin and human carcinogen. Lipids have a variety of important physiological functions and the abnormal lipid metabolism has been reported to be closely related to the occurrence and development of many diseases. In the present study, we aim to utilize LC-MS/MS lipidomic platform to identify novel biomarkers and provide scientific clues for mechanism study of benzene hematotoxicity. Results showed that a total of 294 differential metabolites were obtained from the comparison of benzene-treated group and control group. The glycerophospholipid pathway was altered involving the down-regulation of the levels of phosphatidylcholine and phosphatidylserine. In addition, phosphatidylethanolamine (PE) and 1-Acyl-sn-glycero-3-phosphocholine levels were increased in benzene-treated group. Based on the relationship between PE and autophagy, we then found that effective biomarker of autophagy, Beclin1 and LC3B, were increased remarkably. Furthermore, following benzene treatment, significant decreases in glucosylceramide (GlcCer) and phytosphingosine (PHS) levels in sphingolipid pathway were observed. Simultaneously, the levels of proliferation marker (PCNA and Ki67) and apoptosis regulator (Bax and Caspase-3) showed clear increases in benzene-exposed group. Based on our results, we speculate that disturbances in glycerophospholipid pathway play an important role in the process of benzene-induced hematopoietic toxicity by affecting autophagy, while sphingolipid pathway may also serve as a vital role in benzene-caused toxicity by regulating proliferation and apoptosis. Our study provides basic study information for the future biomarker and mechanism research underlying the development of benzene-induced blood toxicity.

Received: 22 February 2021; Revised: 30 April 2021; Accepted: 24 May 2021

© The Author(s) 2021. Published by Oxford University Press. All rights reserved. For Permissions, please email: journals.permissions@oup.com

Graphical Abstract



Key words: benzene; hematotoxicity; lipidomic; glycerophospholipid; sphingolipid pathway

Introduction

Benzene is a class of aromatic compound with a wide range of applications in industrial and chemical manufacturing, such as rubbers, dyes, shoes and automobiles. As a known carcinogen, benzene is associated with a variety of adverse health effects, such as myelodysplastic syndrome and leukemia. Chronic benzene poisoning caused by occupational exposure in many developing countries has become one of major public health concerns [1, 2]. In addition, although the level of environmental benzene exposure among the general population is far lower than that of those exposed in the occupational workplace, it occurs occasionally that childhood leukemia or other hematological diseases caused by inhalation of decoration solvents (such as paint and glue) containing benzene or toluene as raw materials [3]. So far, although many scholars have done extensive experiments and population studies, there is still a lack of specific biomarker related with early hematopoietic injury caused by benzene exposure [4, 5]. Therefore, there is an urgent need to find novel biomarkers involved in benzene-induced hematopoietic toxicity and provide scientific basis for the early identification and prevention of benzene toxicity.

Lipids are a fundamental part of the biofilm, as well as the metabolites of organisms, which play a crucial role in cell energy storage, composition and signal transduction. In recent years, some studies have shown that lipids are potential biomarkers for multiple diseases [6]. Kouba et al. [7] reported that lysophosphatidic acid and arachidonic acid (AA), two kinds of lipids, were

at high concentrations in epithelial ovarian cancer patients and related to proliferation and migration of cancer cells. According to previous research, six specific lipids including phosphatidylcholine (PC) (20: 2/20: 5ay) serve as potential biomarkers for early diagnosis of breast cancer [8]. Additionally, the role of lipids in disease has been widely investigated, with particular emphasis on the relevant to blood system diseases. Recent studies have shown that the level of $\text{PGF}2\alpha$ was elevated in the plasma as well as bone marrow (BM) in patients with acute myeloid leukemia (AML) [9]. Usman et al. [10] have reported that total cholesterol and low-density lipoprotein levels were significantly decreased in male participants of the AML population. Given the important role of lipids in hematological diseases, investigation of disturbances in lipids caused by benzene exposure may provide novel insights into the potential biomarker finding.

Since the crucial role of lipids in cell, tissue and organ physiology, there has been increased interest in research aimed at lipid role in the occurrence and development of various diseases and mechanism studies. As a comprehensive analysis of the lipid system of the body, lipidomics now has developed into a holistic research method to qualitatively and quantify lipid metabolite. Lipidomics analysis is helpful for molecular mechanism study through a serial of procedures: sample preparation, data acquisition, data processing and data interpretation [11, 12]. Furthermore, the pathways and networks of lipid metabolism were used to identify the molecular mechanisms responsible for disease pathogenesis [13]. Yang et al. [14] have found that abnormal glycerophospholipid metabolism pathway

may be associated with lipid metabolism disorder caused by hyperuricemia through lipidomic investigation. Wu *et al.* [15] found that phospholipid metabolism may relate to the process of regulating Huang-Qi-San for treating early type 2 diabetes based on UPLC/Q-TOF-MS lipidomic method. Hence, it is reasonable to use lipidomics to study the mechanism of benzene-induced hematopoietic toxicity.

Previous studies from our lab reported that 150-mg/kg benzene caused hematotoxicity [16]. In this study, we compared BM lipidomic profiles in control mice and 150-mg/kg benzene exposure mice using LC-MS/MS technology. OPLS-DA was performed to identify differential lipids. Results showed that a total of 294 lipids identified could be used as potential biomarkers. Furthermore, glycerophospholipid metabolism and sphingolipids metabolism were deregulated in benzene-treated group through Metabolic Pathway Analysis (MetPA). To investigate the role of glycerophospholipid metabolism and sphingolipids metabolism in benzene toxicity, we assessed the expression of key enzymes and cellular physiology-related genes. Our research in identification of benzene exposure-associated lipids and biological pathways may provide new clues for finding early screening biomarkers and mechanism research of benzene-induced hematotoxicity.

Materials and Methods

Materials

Benzene was produced by Sigma Co. (St. Louis, USA). HPLC grade acetonitrile, methanol, water and isopropanol were obtained from CNW Technologies GmbH (Dusseldorf, Germany). L-2-chlorophenylalanine was obtained from Hengchuang Biotechnology Co., Ltd (Shanghai, China).

Methods

Animal treatment. The study protocols were approved by the Research Ethics Committee of Southeast University (Nanjing, China, approve number: 20181224006). Male C57BL/6 mice with an initial body weight of 20 ± 3 g (aging $\sim 7 \pm 1$ weeks) were kept in specific pathogen-free houses ($23 \pm 1^\circ\text{C}$, with a relative humidity of $50 \pm 10\%$ and a 12-hour light/dark cycle). There were 6 mice in each cage. All mice have free access to sterile food and water and adapt to these conditions for a week before starting the experiment. Based on our previous study [16], mice were subcutaneously injected with 150-mg/kg benzene, once a day for 30 days. Another group of randomly assigned mice served as the untreated controls. Each group contained 6 mice. The weight of mice was checked every other week. At the end of the treatment cycle, mice were euthanised by cervical dislocation. The BM cells were harvested from the four murine limbs.

Sample preparation. Mouse BM cells were collected and transferred to a 1.5-ml sterile Eppendorf tube. Two small steel balls were added into each tube. Twenty microlitre of internal standard (0.3 mg/ml of L-2-chlorophenylalanine dissolved in methanol) and 600 μl of methanol/water mixture (4/1, v/v) were added into each sample. Then, 600 μl of chloroform was added and the mixture was ultrasonicated on ice for 6 min. All solution was transferred into a pointed glass centrifuge tube and extracted with ultrasonication in an ice-water bath for 10 min. After centrifugation at 7500 rpm at 4°C for 10 min, the lower layer of liquid was injected into a GC-MS vial and vacuum dried. Then, 600 μl of chloroform/methanol (2/1, v/v) was added into upper layer of

liquid, vortexed for 30 s and ultrasonicated in an ice-water bath for 10 min. Again, the solution in lower layer was put into the treated upper layer sample vial and dried using a centrifugal vacuum evaporator. The lipid extracts were reconstituted in 600 μl of isopropanol/methanol (1/1, v/v) and centrifuged at 13 000 rpm for 10 min at 4°C . Finally, 200 μl of supernatant was prepared for LC-MS/MS analysis. The quality control sample was a mixture taken from each sample with equal volume.

LC-MS/MS-based lipidomics analysis. The LC-MS/MS lipidomics analysis was carried out on a Nexera UPLC (Shimadzu, Kyoto, Japan) coupled to a Q Exactive mass spectrometer (Thermo Scientific™). An ACQUITY UPLC BEH C18 column (1.7 μm , 2.1×100 mm) was used in both positive and negative modes. The column was maintained at 45°C and the flow rate was 0.35 ml/min. The mobile phase was: (A) acetonitrile: water = 6:4 (v/v), (B) acetonitrile: isopropanol = 1:9 (v/v). Both solvent A and B were added with 10 mmol/l ammonium formate and 0.1% formic acid. The gradient was 0–3 min maintained at 30% B; 3–5 min from 30 to 62% B; 5–15 min from 62 to 82% B; 15–16.5 min to 99% B and maintained for 1.5 min; and 18.1 min reduced to 30% B and maintained for 3.9 min. The whole process took 22 min. The mass parameters were set as follows: heater temperature, 300°C ; sheath gas flow rate, 45 arb; aux gas flow rate, 15 arb; sweep gas flow rate, 1arb; capillary temperature, 320°C ; S-Lens RF level, 50%; the spray voltage was set at 3.5 KV in positive mode and 3.1 KV in negative mode, respectively. The MS1 scan range was from 120 to 1800. The mass-to-charge ratio of lipid molecules and lipid fragments was collected as follows: 10 fragment maps (MS2 scan, high-energy collisional dissociation) were acquired after each full scan. The resolution of MS1 was 70 000 and MS2 resolution was 17 500 (at m/z 200). The QC samples were injected every six samples throughout the analytical run.

Multivariate data processing. The raw data were collected by UNIFI 1.8.1. software and then analyzed using Progenesis QI v2.3 software (Nonlinear Dynamics, Newcastle, UK). The peak identification, lipid identification, peak extraction and alignment and quantification were proceeded. Following parameters were used: precursor tolerance: 5 ppm; product tolerance: 5 ppm and product ion threshold: 5%. After Progenesis QI analysis, compounds were identified based on accurate masses, secondary fragments and isotopic distributions using the Lipidmaps (v2.3) database. For the extracted data, the lipid molecules with >50% missing values in the group were deleted. Multidimensional statistical analysis was conducted using SIMCA-P 14.1 (Umetrics, Umea, Sweden), including unsupervised principal component analysis (PCA) analysis, supervised exclusion least squares discriminant analysis (PLS-DA) and orthogonal partial least squares-discriminant analysis (OPLS-DA). Based on the OPLS-DA, the variable importance plot (VIP) > 1 was selected, and the *P*-value of the student's *t* test <0.05 was considered to be significantly different.

Metabolite annotation and pathway analysis. To gain the metabolic pathway enrichment analysis associated with benzene treatment, differential lipids were assessed by MetaboAnalyst 5.0 (<http://www.metaboanalyst.ca>) online software. In detail, metabolic pathway was calculated by differentially expressed lipids detected in both ion modes. MetaboAnalyst is a free database to disclose metabolic pathway. The combination of powerful path enrichment analysis results and topological analysis gives MetaboAnalyst an advantage. MetPA (Metabolomic

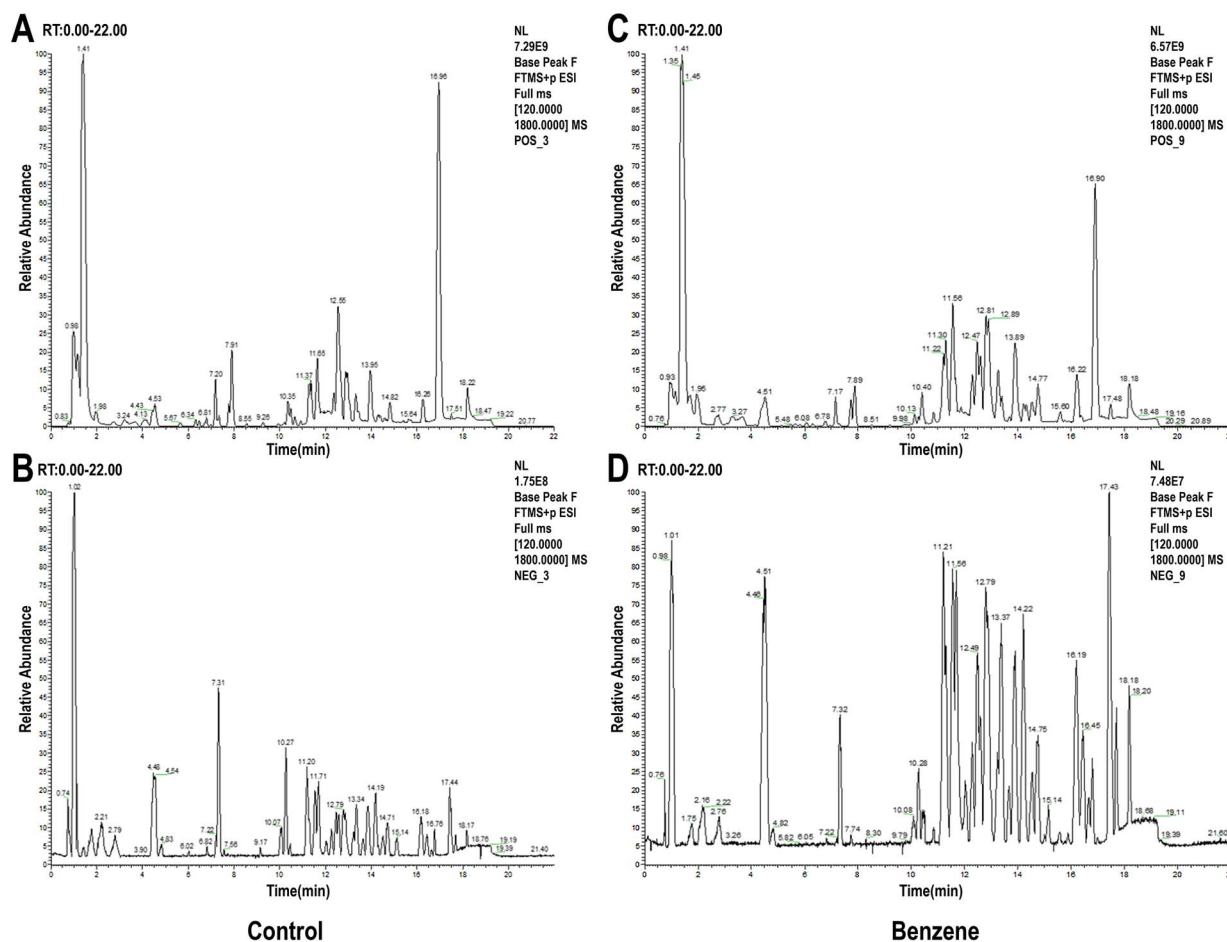


Figure 1: typical BPC of mouse BM cells in control and benzene group on positive (A and B) and negative mode (C and D); (A, C) control group; (B, D) benzene group.

Pathway Analysis) can identify pathways that are significantly changed under specific experimental conditions.

RNA isolation and qRT-PCR. Total RNA was extracted using the Trizol method. The reverse transcriptase Takara Taq kit (Takara Bio, Shiga, Japan) was used to generate cDNA. Specific primers (Genery, Shanghai, China) were used to perform qRT-PCR on the cDNA. The qPCR procedure was designed under the following conditions: was 95°C for 5 s, then 40 cycles of 95°C for 15 s, 60°C for 60 s and 95°C for 15 s. The relative expression level of the gene was normalized to β -actin. The primer was showed in Table 1. All the samples were done in duplicates, three independent times. The $2^{-\Delta\Delta Ct}$ method was calculated the relative gene expression.

Statistical analysis. All data were statistically analyzed by a two-tailed Student's t test using SPSS 22.0 statistical software. The quantitative data were expressed as means \pm SD. $P < 0.05$ was considered statistically significant.

Results

Benzene exposure caused hematotoxicity

Our previous studies shown that mice exposed to 150-mg/kg benzene had significant hematopoietic damage compared with control mice [16]. The results have reported that levels of white blood cell were decreased remarkably in 150-mg/kg benzene

exposed group. In addition, red blood cell level and hemoglobin levels were altered significantly. Furthermore, benzene exposure also decreased the percentage and the colony forming capability of hematopoietic stem cells (HSCs) [17, 18].

Comparative analysis between the control and benzene groups

Base peak chromatograms (BPC) of mouse BM cells in control and benzene group on positive and negative modes are shown in Fig. 1. The PCA and OPLS-DA analyses were established to reveal the difference between control and benzene group using multivariate statistical analysis. As shown in Fig. 2, OPLS-DA score plot revealed more clear discrimination between two groups than PCA plot, with a R^2Y value of 0.993 and a Q^2 of 0.825, respectively. The results indicated that we could acquire more reliable metabolites information resulted in significant differences between the two sets of samples after effective elimination of the noise and uncorrelated variation. To test the validity of the OPLS-DA model, we performed permutation test with 200 random permutations in OPLS-DA model. The extrapolated intercept value (Q_{2inter}) was -0.145 (negative), demonstrating that the statistical model was validated and no over-fitting was observed.

Screening of differential lipid metabolites

Herein, based on the OPLS-DA analysis, 294 lipids with $VIP \geq 1$ were selected and further confirmed by a student's t test

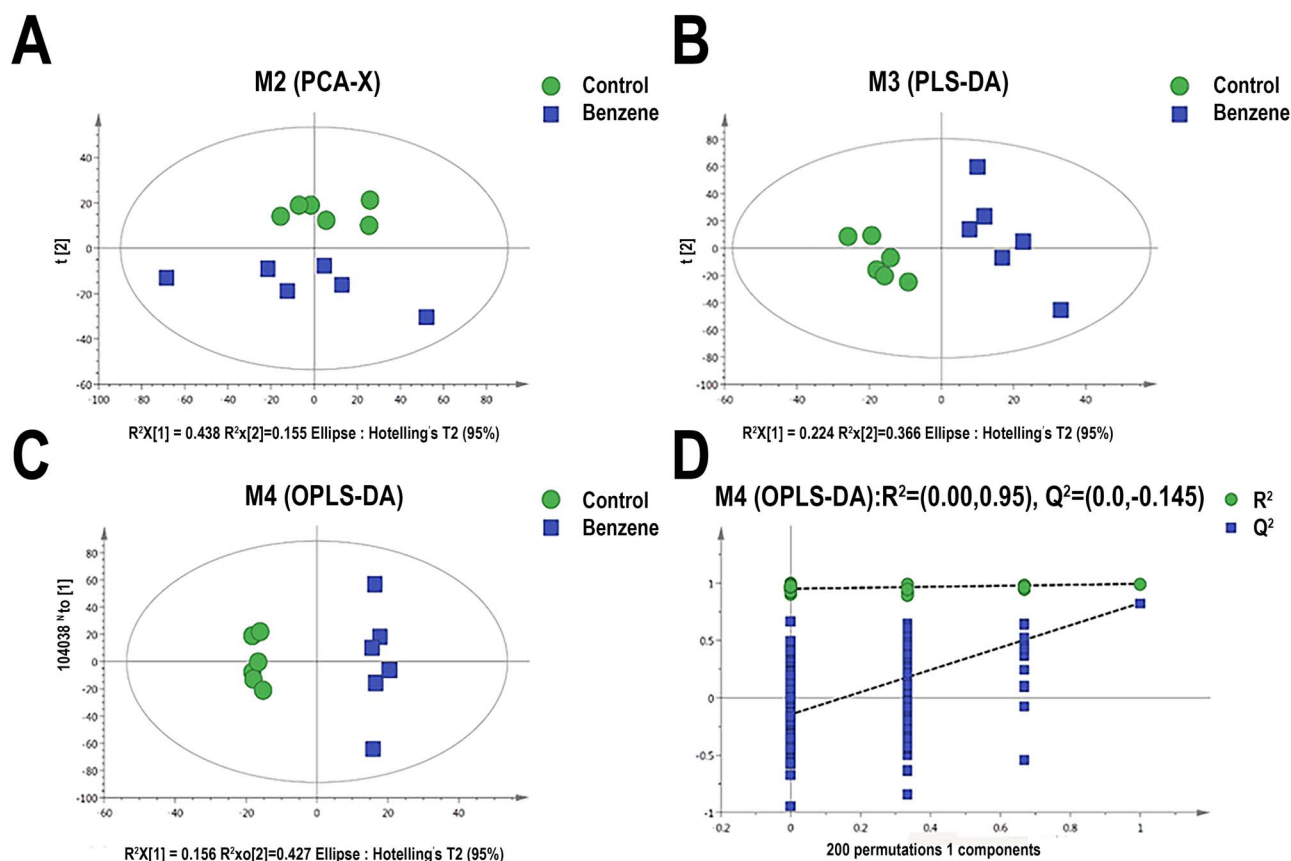


Figure 2: models derived from LC-MS dataset of BM cells from control and benzene group; (A) score plots of the PCA models; (B) supervised exclusion least squares discriminant analysis (PLS-DA); (C) orthogonal partial least squares-discriminant analysis (OPLS-DA); (D) permutation test ($n = 200$) validation plots of the OPLS-DA models; each point in the figure represents a single sample; green dots represent mice in control group; blue boxes represent samples in benzene exposure group.

Table 1: primers used in the article

	Gene	Primer (5'-3')
mouse	Actin	F ¹ -CCTCACTGTCCACCTTCC; R ² -GGGTGTAAACGCAGCTC
mouse	cept1	F-AGACACCAGTTAAACGGCTA; R-GGCAATCCATGAGGGTACT
mouse	chpt1	F-GGTAAAGGCGCTAGGTGAG; R-GCAGCCAGGTCCAGTAAA
mouse	pisd	F-CCAACGAGTTTGTCTGTAT; R-TCACCCCAAAGTCCAG
mouse	ptdss1	F-TCCTGTTGTGCAATGGTG; R-TGGTGTGGATGTCCTTGA
mouse	ptdss2	F-AAGCTAAAGACGGGCCATT; R-AGAAACTGTCGGCCATCC
mouse	Lcat	F-GCGGGATGAGACAGTGC; R-ACAGGCTTCCATAAGCG
mouse	Degs1	F-AGTGATGCTCGGAAGCTG; R-TGAGTGCAGGGGAGTGA
mouse	UGCG	F-AATGTGTGACGGGGATGT; R-CAACCTCGGTCGGCTAT
mouse	LC3B	F-CAGCCACACCCTTTCCT; R-GTCAGCAACCCCTGGAC
mouse	Beclin1	F-ATTGAAGACACTGGAGGCA; R-CAGGCAAGACCCCACTT
mouse	Bax	F-GCCTCCTCTCTACTTCCG; R-TCAGCCCATCTTCTTCCAG
mouse	Bcl-2	F-ACAAGTGCCTGCTTTATGG; R-CTGCTCTGTTCCAAACCC
mouse	Caspase-3	F-TGTGCTAGAAACGAAAGGG; R-CCATAAGGAGGCCAGGA
mouse	PCNA	F-TCCTGTTGTGCAATGGTG; R-TGGTGTGGATGTCCTTGA
mouse	Ki67	F-TCCAGTGAAGGAGAAGCAG; R-TGATGGGCTCAGGTATGTC

F¹: Forward primer;

R²: Reverse primer.

($P < 0.05$). These lipids include five categories, namely 128 fatty Acyls, 133 Glycerophospholipids, 16 Glycerolipids, 16 Sphingolipids and 1 Sterol Lipids. Glycerophospholipids contributes the most to it, including PC, Phosphatidic acid (PA), phosphatidylethanolamine (PE), phosphatidylinositol (PI), phosphatidyl glycerol (PG) and phosphatidylserine (PS). The

percentage distribution of the four main lipid types was shown in Fig. 3. Furthermore, top 50 significantly changed metabolites were identified as shown in Table 2 with their retention time (RT, min), ion mode, metabolite, molecular formula, VIP value, P-value and related trends. The result showed that 30 lipid metabolites were significantly up-regulated in benzene-exposed mice, while

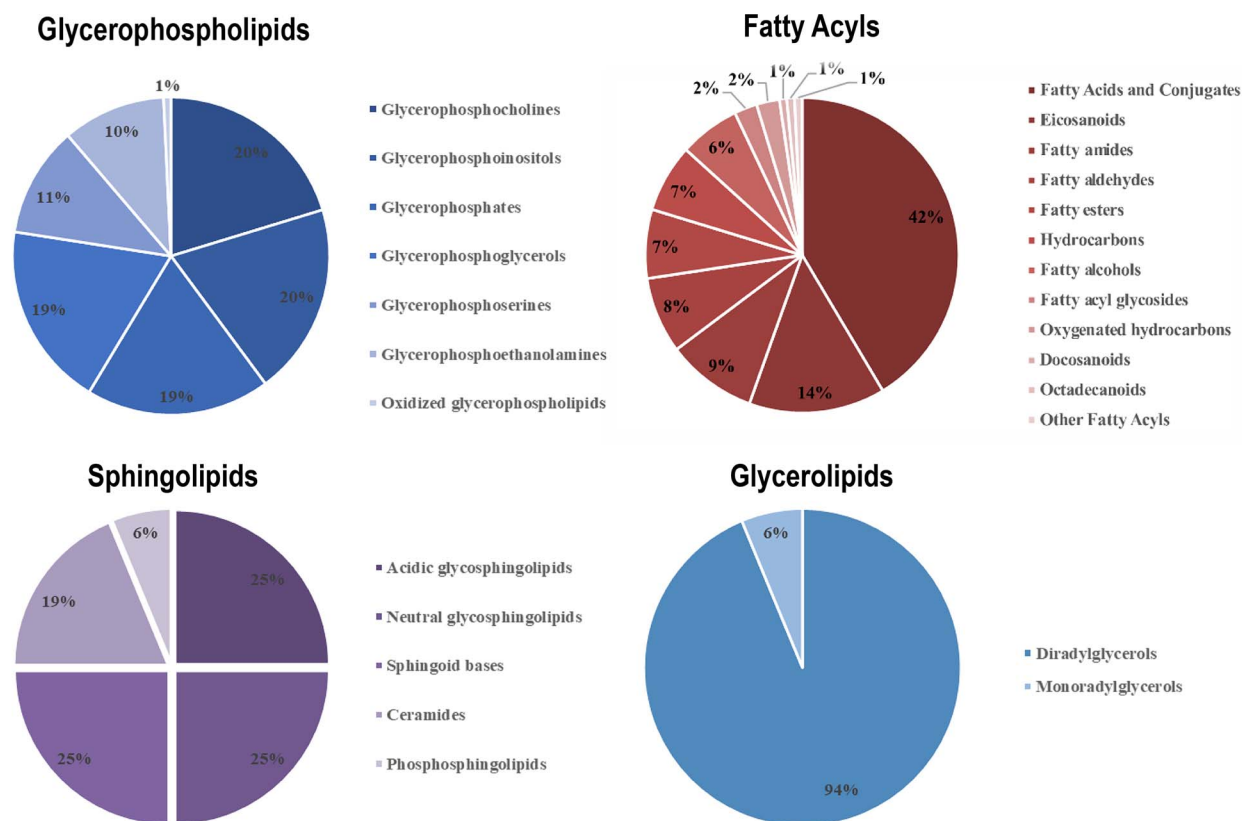


Figure 3: the proportional contribution of subclass lipids in four categories; lipidomic profiling revealed 294 differential lipids distinguishing benzene-treated mice from control mice; these lipids were distributed in four main lipid types, namely fatty acyls, glycerophospholipids, glycerolipids and sphingolipids.

20 lipid metabolites were down-regulated. Additionally, the clustering heat map also observed distinct segregation between benzene-treated group and control group (Fig. 4).

Metabolic pathway analysis

Metabolic pathway enrichment analysis in mice with benzene exposure was identified by MetaboAnalyst 5.0 (<http://www.metaboanalyst.ca>) software. The 294 metabolites with obvious changes were imported to MetPA for the metabolic pathway analysis. As shown in Fig. 5A, the results were presented with form of interactive visualization system. A total of 15 metabolic pathways were affected by benzene exposure and the detailed results of top five pathways analysis were shown in Table 3. The *P*-value threshold calculated from pathway topology analysis was set to 0.05. Two cardinal metabolic pathways were discovered, namely glycerophospholipid metabolism and sphingolipids metabolism with *P*-value at 0.00, 0.04, respectively. Metabolic network was constructed shown in Fig. 5B and C.

The glycerophospholipid pathway may involve in benzene-induced blood toxicity via influencing autophagy

Among them, glycerophospholipid metabolism was the pathway with the most significant enrichment level ($-\log(P) = 2.75$, Raw *P* = 0.00). The alterations of significantly changed lipid

metabolites in glycerophospholipid metabolism and their corresponding regulation genes were shown in Fig. 6A. As shown in Fig. 6B, PC and PS were down-regulated in benzene exposure group. PE and 1-Acyl-sn-glycero-3-phosphocholine were significantly increased compare with control group ($P < 0.05$). We then detected the expression of key enzymes of glycerophospholipid metabolism (Fig. 6C). PS decarboxylase (psid) enzyme converts PS to PE in the inner mitochondrial membrane. Cholesterol acyltransferase (Lcat) transfer an acyl group from lecithin to cholesterol. In mammals, PtdSer synthase enzymes, ptdss1 and ptdss2, utilize PC and PE as substrates to synthesize PS, respectively. We found that mRNA levels of psid, ptdss1 and ptdss2 showed a significant decline, while Lcat was presented higher level in benzene-treated group. Because PE has been reported to play a key role in autophagosome biogenesis [19]. We then also explored whether the changes in PE were coupled with alterations in autophagy. The results showed that Beclin1 and LC3B, two autophagy-related genes, were elevated in benzene-exposed mice (Fig. 6D) ($P < 0.05$). Hence, the glycerophospholipid pathway may involve in benzene-induced hematopoietic toxicity by partially increasing cell autophagy.

Sphingolipid pathway may participate in benzene-induced blood toxicity by regulating cell proliferation and apoptosis

Sphingolipids metabolism was also a vital pathway associated with metabolic changes in benzene-exposed mice ($-\log(P) = 1.40$, Raw *P* = 0.04). Figure 7A displayed the regulation relationship

Table 2: top 50 identified differential lipids based on VIP & P-value

NO.	m/z	RT ¹ (min)	Ion mode	Metabolites	Formula	VIP ²	P-value	Trend (B/C)
1	245.1741	1.52	pos	2-methyl-dodecanedioic acid	C13H24O4	2.26	5.72E-05	down
2	169.9855	0.76	pos	Iminospartic acid	C4H5NO4	2.41	1.83E-06	down
3	134.1174	0.76	pos	4-hydroxy caproaldehyde	C6H12O2	2.33	2.11E-05	down
4	14.0680	0.78	pos	2S-amino-pentanoic acid	C5H11NO2	2.42	1.45E-06	down
5	162.1485	0.76	pos	Butan-2-one	C4H8O	2.37	8.36E-06	down
6	232.1539	0.76	pos	O-butanoyl-carnitine	C11H21NO4	2.46	4.40E-08	down
7	132.1018	0.80	pos	2S-amino-hexanoic acid	C6H13NO2	2.31	3.33E-05	down
8	16.1329	0.76	pos	cis-epsilon-octenoic acid	C8H14O2	2.35	1.59E-05	down
9	209.1505	0.76	pos	Undecylic acid	C11H22O2	2.44	8.75E-08	down
10	859.6047	7.53	pos	PI(O-16:0/22:2(13Z,16Z))	C47H89O12P	2.41	6.55E-07	down
11	918.6436	8.30	pos	PI(O-18:0/22:4(7Z,10Z,13Z,16Z))	C49H89O12P	2.08	1.38E-03	down
12	873.5845	12.66	pos	PI(O-20:0/18:4(6Z,9Z,12Z,15Z))	C47H85O12P	2.00	2.19E-03	down
13	893.5489	11.12	pos	PI(O-18:0/20:5(5Z,8Z,11Z,14Z,17Z))	C47H83O12P	2.13	6.27E-04	down
14	846.5420	11.42	pos	PC(18:4(6Z,9Z,12Z,15Z)/20:1(11Z))	C46H82NO8P	2.01	1.41E-03	down
15	822.5021	7.43	pos	PC(18:4(6Z,9Z,12Z,15Z)/20:5(5Z,8Z,11Z,14Z,17Z))	C46H74NO8P	2.05	1.43E-03	down
16	340.3932	6.22	pos	5Z-Tricosene	C23H46	2.02	1.92E-03	down
17	767.4092	6.73	pos	Ustilagic acid	C36H64O18	2.01	1.28E-03	down
18	457.2575	1.61	pos	PG(14:0/0:0)	C20H41O9P	2.01	2.21E-03	down
19	368.4244	7.11	pos	5Z-Pentacosene	C25H50	2.03	1.78E-03	down
20	739.3790	6.32	pos	15-keto-PGE2	C20H30O5	2.19	2.18E-04	down
21	692.5964	18.72	pos	PE-NMe2(O-16:0/O-16:0)	C39H82NO6P	2.50	3.21E-10	up
22	374.3773	11.14	pos	6-Ethyl-4-methyl-3E,5E,7E-decatriene	C13H22	2.18	2.47E-04	up
23	688.4326	10.63	pos	PC(10:0/16:0)	C34H68NO8P	2.01	1.61E-03	up
24	127.0387	1.01	pos	(E)-hex-2-enedioic acid	C6H8O4	2.17	4.37E-04	up
25	135.0800	1.15	pos	2,6Z-Nonadien-4-olide	C9H12O2	2.17	3.13E-04	up
26	219.1740	7.60	pos	6,8,10,12-pentadecatetraenal	C15H22O	2.11	5.01E-04	up
27	387.1794	10.65	pos	10-oxo-5,8-decadienoic acid	C10H14O3	2.02	1.79E-03	up
28	468.5135	14.07	pos	3S,11S-Dimethylnonacosan-2-one	C31H62O	2.06	1.20E-03	up
29	454.2915	6.79	pos	PA(18:1(9Z)/0:0)	C21H41O7P	2.36	6.34E-06	up
30	319.2260	1.14	pos	9-hydroxy-2Z,5E,7Z,11Z,14Z-Eicosapentaenoic acid	C20H30O3	2.06	1.38E-03	up
31	351.1584	1.75	pos	PA(6:0/6:0)	C15H29O8P	2.01	2.16E-03	up
32	414.2972	5.83	pos	N,N-(2,2-dihydroxy-ethyl) arachidonoyl amine	C24H41NO3	2.38	4.11E-06	up
33	397.2002	1.75	pos	8-oxo-Resolvin D1	C22H30O5	2.02	1.66E-03	up
34	291.2286	34	pos	2R-aminooheptanoic acid	C7H15NO2	2.28	3.03E-05	up
35	675.5888	18.55	pos	DG(20:0/18:0)	C41H80O5	2.26	9.95E-05	up
36	34.2813	1.38	pos	Phytosphingosine	C18H39NO3	2.05	1.35E-03	up
37	633.5421	17.63	pos	DG(15:0/20:0/0:0)[iso2]	C38H74O5	2.10	1.05E-03	up
38	356.3516	6.13	pos	Eicosanoyl-EA	C22H45NO2	2.02	2.97E-03	up
39	785.5034	9.51	pos	3-O-(2-O-(2E-decenoyl)-alpha-L-rhamnopyranosyl)-(1-2)-alpha-L-rhamnopyranosyl)-3-hydroxydecanoic acid	C42H74O14	2.23	3.47E-04	up
40	470.4200	9.05	pos	5-methyl-2E-tridecenoic acid	C14H26O2	2.19	4.05E-04	up
41	646.4801	9.12	pos	PE(P-16:0/14:1(9Z))	C35H68NO7P	2.08	1.56E-03	up
42	768.4758	8.84	pos	PS(16:0/17:2(9Z,12Z))	C39H72NO10P	2.13	8.09E-04	up
43	532.3366	4.04	pos	PC(O-10/16:0)	C25H52NO7P	2.13	6.32E-04	up
44	757.6472	18.19	pos	PA(O-20:0/22:0)	C45H91O7P	2.22	3.61E-04	up
45	699.5943	9.00	pos	DG(20:5(5Z,8Z,11Z,14Z,17Z)/22:0/0:0)[iso2]	C45H78O5	2.21	2.76E-04	up
46	431.2160	0.94	pos	PA(16:1(9Z)/0:0)	C19H37O7P	2.15	6.70E-04	up
47	646.4803	8.58	pos	PC(17:0/10:0)	C35H70NO8P	2.16	7.60E-04	up
48	630.4515	8.07	pos	PC(12:0/14:1(9Z))	C34H66NO8P	2.13	8.44E-04	up
49	566.4753	7.53	pos	DG(13:0/18:3(9Z,12Z,15Z)/0:0)[iso2]	C34H60O5	2.13	1.03E-03	up
50	494.3236	2.24	pos	PC(16:1(9E)/0:0)	C24H48NO7P	2.28	7.82E-05	up

RT¹: retention time;VIP²: the variable importance of the projection.

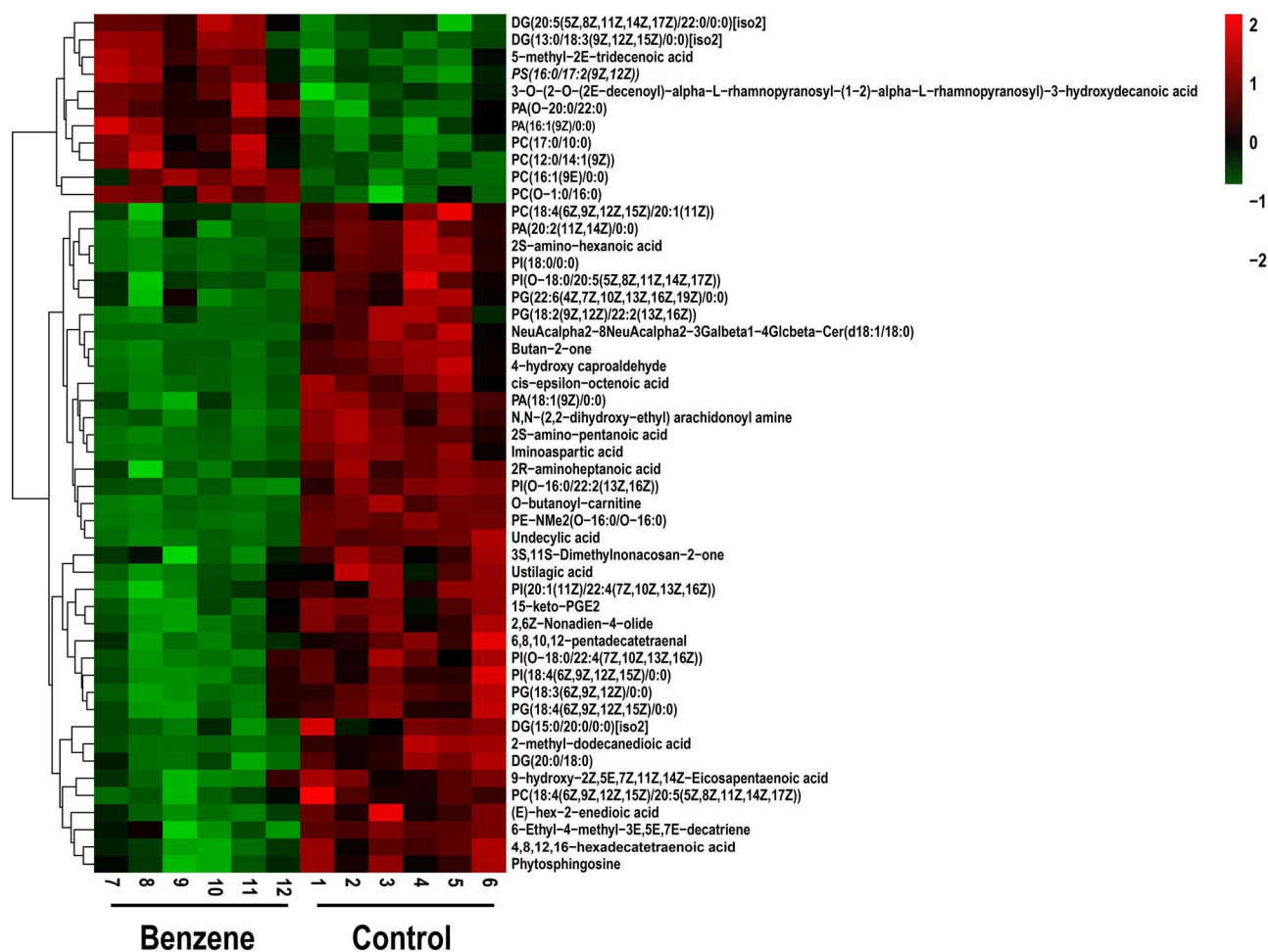


Figure 4: hierarchical clustering heat map of the top 50 differential lipid; each column represents an individual sample from benzene-exposed group (7–12) and control group (1–6); each row represents a kind of lipid; the degree of change is marked by different colors, and red represents the up-regulation, green represents the down-regulation

Table 3: result from pathway analysis

NO	Pathway name	Total compounds ¹	Hits ²	Raw(P) ³	Log(P) ⁴	Holm(P) ⁵	FDR p ⁶	Impact ⁷
1	Glycerophospholipid metabolism	36	4	0.00	2.75	0.14	0.14	0.26
2	Sphingolipid metabolism	21	2	0.04	1.40	1.0	1.0	0.04
3	Linoleic acid metabolism	5	1	0.07	1.12	1.0	1.0	0.00
4	AA metabolism	36	2	0.10	0.98	1.0	1.0	0.00
5	Biosynthesis of unsaturated fatty acids	36	2	0.10	0.98	1.0	1.0	0.00

Tota¹: the total number of compounds in the pathway;

Hits²: the actually matched number from the user uploaded data;

Raw (p)³: the original p value calculated from the enrichment analysis;

Holm (p)⁴: the p value adjusted by Holm-Bonferroni method;

FDR p⁵: the p value adjusted using False Discovery Rate;

Impact⁶: the pathway impact value calculated from pathway topology analysis.

between the significantly altered sphingolipids metabolites and key genes caused by benzene exposure. Two lipids in sphingolipids metabolism, glucosylceramide (GlcCer) and phytosphingosine (PHS), were clearly lower in benzene-exposed group (Fig. 7B) ($P < 0.05$). We then detect the expression level of key genes in sphingolipids metabolism. UDP-glucose ceramide

glucosyltransferase (UGCG) encodes a key regulatory enzyme which regulates GlcCer. Delta 4-desaturase, sphingolipid 1 (Degs1) is an ER-membrane-spanning protein, which converts dihydroceramide (dhCer) to Cer. Compared with control group, UGCG and Degs1 gene displayed a considerable elevation in benzene-treated group (Fig. 7C) ($P < 0.05$). Studies have shown

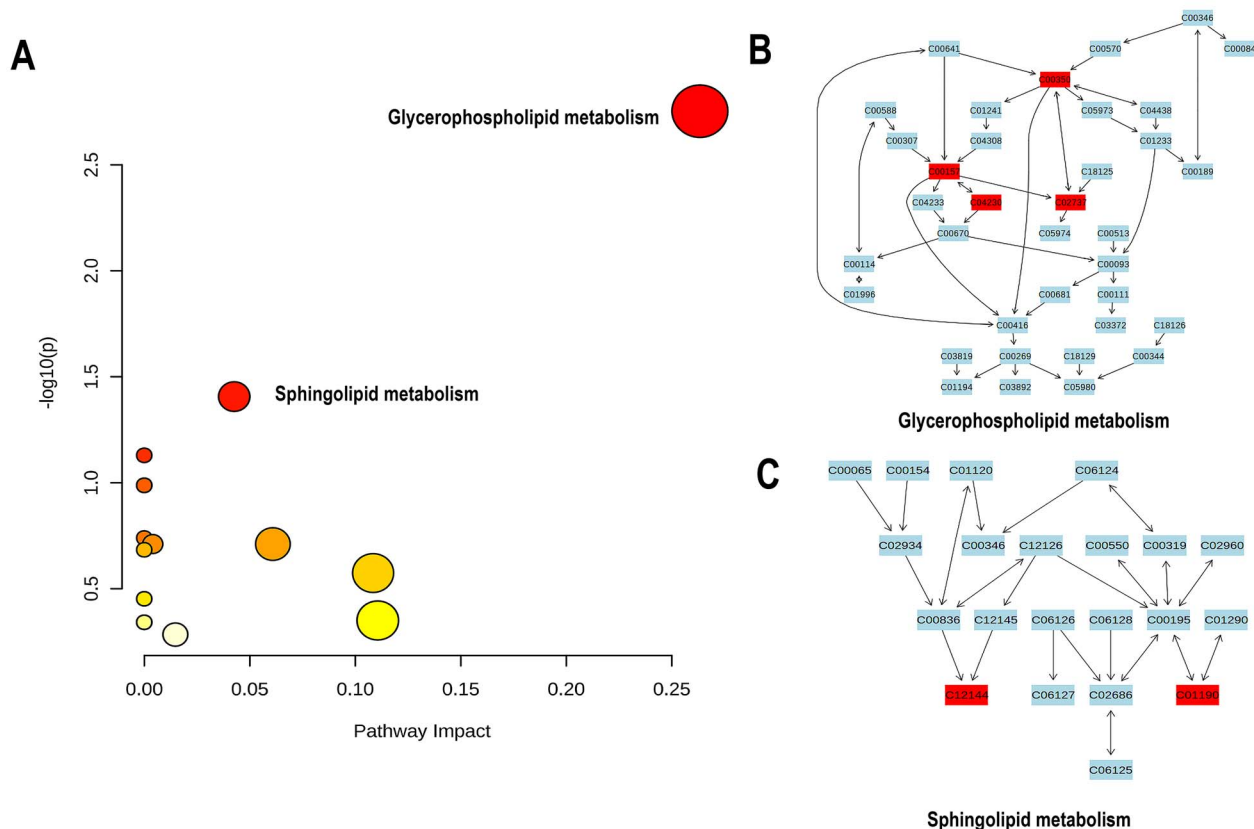


Figure 5: metabolic pathway enrichment map; (A) summary of pathway analysis using MetPA; results from pathway analysis are presented in Table 3. Axis x represented pathway impact score (the larger the circle the higher the impact score), axis y showed the P-value (yellow: higher P-value and red: lower P-value), respectively; (B and C) detailed construction of the glycerophospholipid metabolism and sphingolipids metabolism; labels within small boxes correspond to KEGG identifiers for metabolites; (C00350 – PE; C00157 – PC; C04230 – 1-Acyl-sn-glycero-3-phosphocholine; C02737 – PS; C12144 – Phytosphingosine (PHS); C01190 – Glucosylceramide (GlcCer)).

that two cellular processes, apoptosis and proliferation, could be regulated by sphingolipids [20]. Thus, we then investigated whether benzene exposure impact apoptosis and proliferation in mouse BM cells. The results showed that proliferating cell nuclear antigen (PCNA) and Ki67, two proliferation markers, were significantly elevated in benzene group compared with control. After treatment with benzene, Bax, and Caspase-3 genes, which are core regulators of the intrinsic pathway of apoptosis, were markedly higher, and Bcl-2 showed a significant decline than that of control (Fig. 7D) ($P < 0.05$). Thus, dysregulation in sphingolipids may play a role in abnormal proliferation and apoptosis induced by benzene.

Discussion

Benzene can cause serious damage to the human hematopoietic system, resulting in varying degrees of pancytopenia, aplastic anemia and leukemia. In the previous study, we reported that benzene exposure cause hematotoxicity which was confirmed by damaging to HSCs and decreasing blood cells counts [18]. Given the complex roles of lipids in cellular physiology, it is clear that deregulated lipids may contribute to disease. Simultaneously, lipidomics is an emerging technique for comprehensively analyzing the end products of lipid metabolism and revealing internal changes within whole organisms. BM is the target organ for benzene, and BM cells are often used as samples to analyze the hematopoietic toxicity caused by benzene. Therefore, in this study, BM cells from benzene-exposed and control mice were

collected for lipid metabolism analysis. Based on the LC-MS/MS technology, the data were obtained and then lipid metabolites were screened through OPLS-DA model and comprehensive multivariate analysis. At the same time, their biological functions and related pathways were identified through MetPA.

After benzene exposure, a total of 294 metabolites were identified. Interestingly, glycerophospholipid metabolism and sphingolipid metabolism emerged as crucial pathways that were deregulate in benzene-exposed mice. Glycerophospholipids are major structural components of biological membranes and act as messengers to participate in signaling regulation. Importantly, researchers have found glycerophospholipid metabolism emerged as a crucial role that was deregulated in the disease progression by comparing the serum of ALL patients and controls [21]. In our study, we found that PE were significantly increased in benzene-treated mouse BM cells, while PC and PS declined significantly. The decreasing of multiple PSs level has observed in malignant lung tissue of non-small cell lung cancer patients [22]. Simultaneously, PS was one of the prominent cancer cell biomarkers. Over expression of PS on cancer cells surface enables them to become biomarker in some species cancer, including pancreatic cancer and lung cancer [23, 24]. Cui *et al.* [25] reported that apoptosis was induced by a reduction of PC synthesis in CHO-MT58 cells. Ptdss1 and ptdss2 were the key enzyme that regulate PS through PE and PC as substrates. According to our data, the decline of ptdss1 and ptdss2 levels may be related with the promotion of apoptosis in mouse BM cells after benzene treatment.

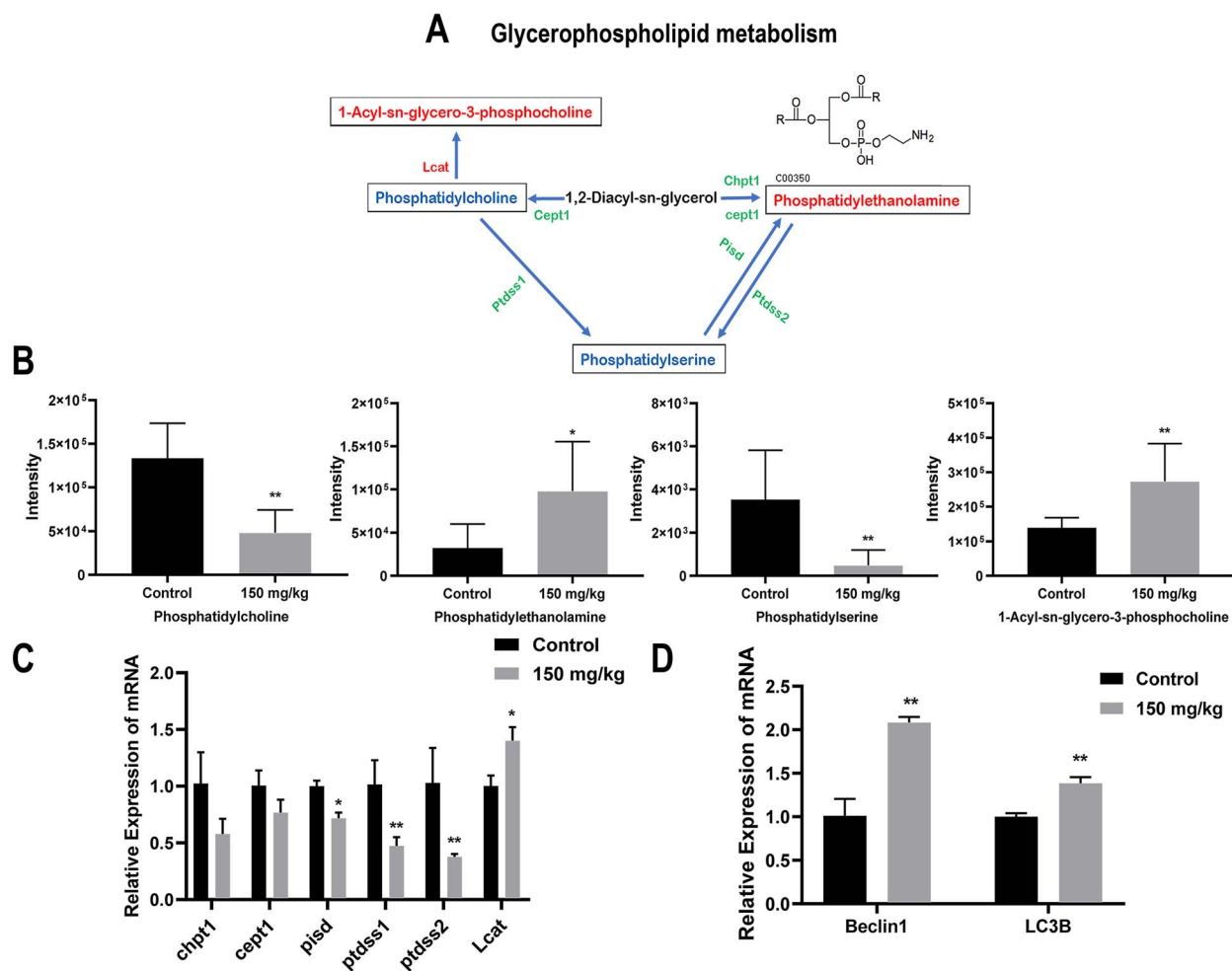


Figure 6: the glycerophospholipid pathway may involve in benzene-induced blood toxicity via influencing autophagy; metabolic pathways of glycerophospholipid metabolism (A); the red and blue words represent the relatively increased or decreased levels of the lipids in solid line box, respectively, and the red and green words on both sides of the solid arrow indicate the up- and down-regulation of the gene expression of the key enzymes; (B) the relative intensity of lipid which were matched in glycerophospholipid metabolism, namely PC, PS, PE and 1-Acyl-sn-glycero-3-phosphocholine, respectively; (C) the expression of each enzyme which may affect lipid levels, including Chpt1, Cept1, PS decarboxylase (Pisd), PtdSer synthase enzymes (Ptdss1and Ptdss2) and Cholesterol acyltransferase (Lcat); (D) the relative mRNA expression of autophagy marker (Beclin1 and LC3B); *: $P < 0.05$; **: $P < 0.01$; ***: $P < 0.001$ compared with control group

Of note, PE has also shown to directly involved in autophagy [26]. LC3-I on the phagophore membrane is conjugated to PE to form LC3-II, which is required for the formation of autophagosomes and selective recruitment of substrates. Both in yeast and in mammalian cell culture, artificial increased intracellular PE level could significantly enhance autophagy level [27, 28]. Increasing evidence demonstrates that deregulated autophagy may be the underlying mechanism by which benzene causes hematotoxicity [29]. In this study, after exposure to 150 mg/kg of benzene for 30 days, two important autophagy genes, namely Beclin 1 and LC3B, were increased in mouse BM cells. Meanwhile, over-expression of Lcat may increase the conversion of PC to 1-Acyl-sn-glycero-3-phosphocholine. Pisd can promote the PE synthesis process on mitochondrial membranes [30]. However, the decreased pisd expression and increased PE level were observed in our study, indicating that there are other metabolic pathways participating in PE synthesis. These results suggest that glycerophospholipid metabolism may be involved in the process of benzene-induced hematopoietic toxicity through regulating autophagy.

Sphingolipids are one of the three major classes of membrane lipids in eukaryotic cells. As important cell signal transduction molecules, sphingolipids metabolites have emerged as key regulators in processes such as cell growth, differentiation, senescence and death. Xie *et al.* [31] have reported that sphingolipid metabolism activated proteostasis programs to govern human HSCs self-renewal. There is sufficient evidence that benzene and its metabolite may act via modulation the self-renewal and differentiation of hematopoietic stem progenitor cells (HSPCs) [32, 33]. Thus, sphingolipid pathway may play an essential role via regulation fuctions of HSPCs in the study of benzene-induced hematopoietic toxicity.

After analyzing the results, GlcCer and PHS in sphingolipid metabolism were significantly decreased in BM cells of mice exposed to benzene in this research. GlcCer is an important glycosphingolipid metabolic intermediate, which serves as the starting point in the biosynthesis of a wide variety of sphingolipids. UGCG is a key enzyme in the sphingolipid metabolism by generating GlcCer, which is the precursor for all complex sphingolipids. Our research showed that the level of GlcCer

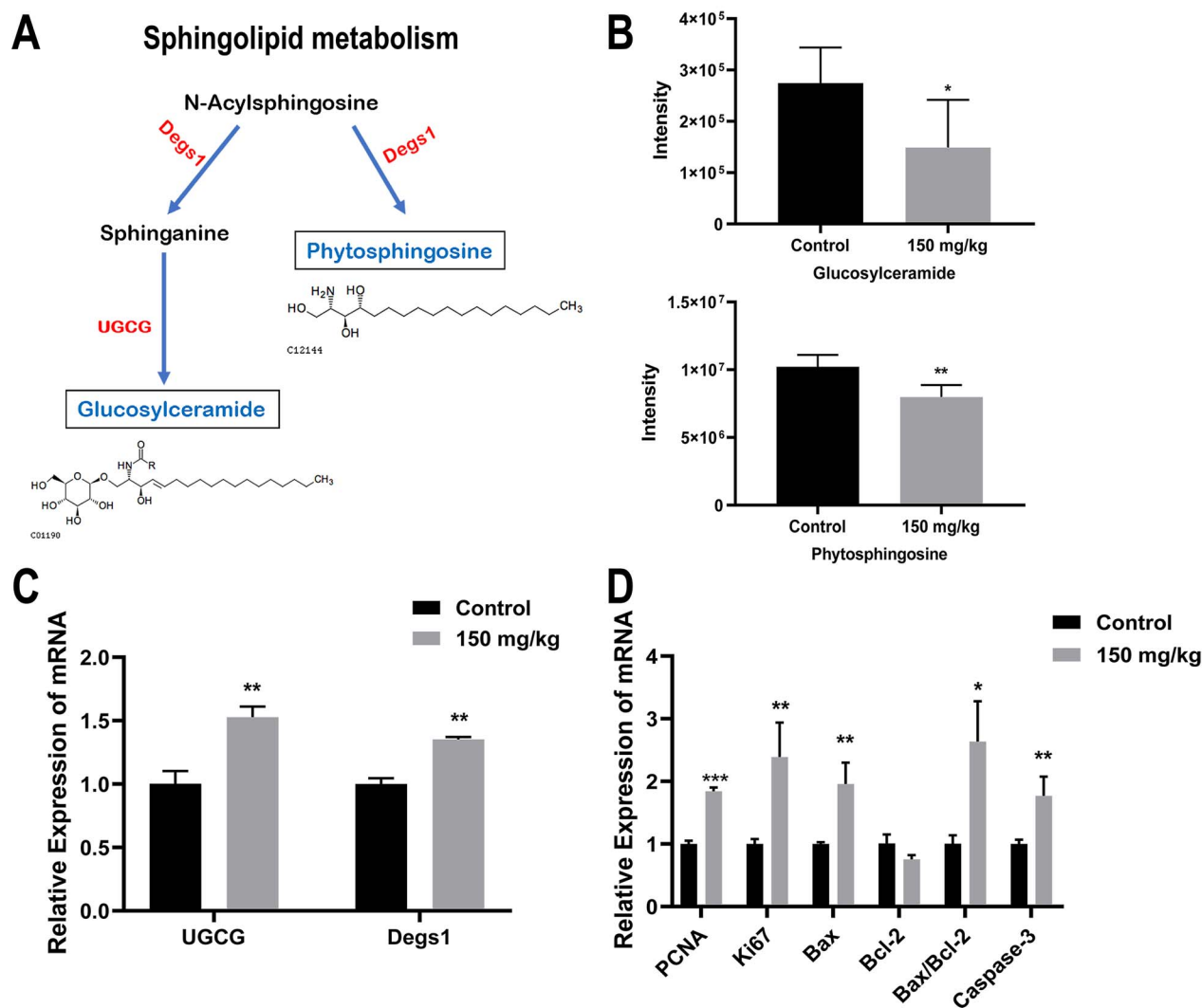


Figure 7: sphingolipid pathway may participate in benzene-induced blood toxicity by regulating cell proliferation and apoptosis; metabolic pathways of Sphingolipids metabolism (A); lipids in solid line box coloured with blue represent the down-regulation of the expression of the metabolites; gene on both sides of the solid arrow were coloured with red represent up-regulation of the expression of enzymes (B); the relative intensity of lipid which were selected in sphingolipids metabolism, including GlcCer and PHS; (C) UGCG and Delta 4-desaturase, sphingolipid 1(*Degs1*) gene expression in mouse BM cells; (D) the relative mRNA expression of proliferation (*Ki67* and *PCNA*) and apoptosis-related genes (*Bax*, *Bcl-2* and *caspase-3*); *: $P < 0.05$; **: $P < 0.01$; ***: $P < 0.001$ compared with control group

was obviously declined after treatment with benzene, but *UGCG* expression level was increased. Chen *et al.* have reported that total GlcCer concentration was significantly lower in MCF-7/*UGCG* over expression cells. These researchers further indicated that the remaining GlcCer were integrated in the cell membrane [34]. *UGCG* is related to pro-cancerous processes such as increased proliferation. Researcher data have showed that an increased *UGCG* mRNA expression can promote MCF-7 cells proliferation [35]. The expression of *UGCG* mRNA and proliferation markers (*Ki67* and *PCNA*) showed an increasing trend with benzene treatment. More experimental studies are needed to verify these assumptions in our study. In addition, the lack of GlcCer may increase the apoptosis of liver cells *in vitro* by *Bcl-2/Bax* pathway [36]. Both *in vivo* and *in vitro* toxicology tests have shown that apoptosis was involved in benzene-induced hematotoxicity by targeting *Bax/Bcl-2* and *Caspase-3* expression [37, 38]. Our results clearly confirmed that benzene promoted

BM cell apoptosis via the upregulation of *Caspase-3* expression and *Bax/Bcl-2* ratio. Based on this result, GlcCer may involve in benzene-induced hematotoxicity via activation of *Bax/Bcl-2*-mediated apoptosis and promoting proliferation.

Of the structural analogs of sphingolipids, PHS is well-known to be involved in many significant cellular responses including apoptosis, differentiation and migration. Han *et al.* [39] have reported that PHS induced several hallmark changes associated with megakaryopoiesis from K562 and HEL cells including cell cycle arrest, cell size increase and polyploidization. The results of scholars have indicated that PHS perturbed mitochondrial functions to induce apoptosis [40]. Our previous study indicated that benzene and benzene metabolites have caused mitochondrial damage, G1 phase accumulation and increases in apoptosis [41–43]. *Degs1*, as a sphingolipid enzyme, is essential for HSCs function [31]. Studies have shown that damage to HSCs played a prominent role in the benzene-induced toxic effect not only

in literatures but also in our previous studies [18, 44, 45]. Our data revealed that PHS level was downregulated in BM cells of benzene-exposed mice and accompanied by *DeGs1* gene changes, suggesting that PHS may participate in benzene-induced hematotoxicity through regulating HSCs self-renewal. Yet, the specific mechanism of PHS in benzene-induced blood toxicity still needs further research.

Conclusion

Taken together, we firstly used BM cell lipidomics to provide new clues for the further study of the mechanism of benzene-induced blood toxicity. However, there are limitations in our study. Firstly, the differential lipids selected by OPLS-DA model are required to be explored at environmental relevant benzene exposure doses. In addition, key potential metabolic biomarkers need to be further validated in occupational population exposed to benzene. As summarized, the present findings do provide the basis for further exploring the mechanism of benzene-induced hematotoxicity.

Acknowledgements

This research was supported by the National Natural Science Foundation of China (81730087, 81703265) and the Fundamental Research Funds for the Central Universities (2242018 K40019, 2242018K3DN25, 2242019R40050).

Conflict of Interest

All authors declare there are no conflicts of interest.

References

- Liu H, Liang Y, Bowes S et al. Benzene exposure in industries using or manufacturing paint in China—a literature review, 1956–2005. *J Occup Environ Hyg* 2009;6:659–70.
- Correa MJ, Santana VS. Occupational exposure to benzene in Brazil: estimates based on an occupational exposure matrix. *Cad Saude Publica* 2016;32:e00129415.
- Bayatian M, Ashrafi K, Azari MR et al. Risk assessment of occupational exposure to benzene using numerical simulation in a complex geometry of a reforming unit of petroleum refinery. *Environ Sci Pollut Res Int* 2018;25:11364–75.
- Liang B, Zhong Y, Chen K et al. Serum plasminogen as a potential biomarker for the effects of low-dose benzene exposure. *Toxicology* 2018;410:59–64.
- Li P, Wu Y, Zhang Z et al. Proteomics analysis identified serum biomarkers for occupational benzene exposure and chronic benzene poisoning. *Medicine (Baltimore)* 2019;98:e16117.
- Sulciner ML, Gartung A, Gilligan MM et al. Targeting lipid mediators in cancer biology. *Cancer Metastasis Rev* 2018;37:557–72.
- Kouba S, Ouldamer L, Garcia C et al. Lipid metabolism and Calcium signaling in epithelial ovarian cancer. *Cell Calcium* 2019;81:38–50.
- Jiang N, Zhang G, Pan L et al. Potential plasma lipid biomarkers in early-stage breast cancer. *Biotechnol Lett* 2017;39:1657–66.
- Pabst T, Kortz L, Fiedler GM et al. The plasma lipidome in acute myeloid leukemia at diagnosis in relation to clinical disease features. *BBA Clin* 2017;7:105–14.
- Usman H, Rashid R, Ameer F et al. Revisiting the dyslipidemia associated with acute leukemia. *Clin Chim Acta* 2015;444:43–9.
- Svegliati-Baroni G, Pierantonelli I, Torquato P et al. Lipidomic biomarkers and mechanisms of lipotoxicity in non-alcoholic fatty liver disease. *Free Radic Biol Med* 2019;144:293–309.
- Afshinnia F, Rajendiran TM, Wernisch S et al. Lipidomics and biomarker discovery in kidney disease. *Semin Nephrol* 2018;38:127–41.
- Kimura T, Jennings W, Epanand RM. Roles of specific lipid species in the cell and their molecular mechanism. *Prog Lipid Res* 2016;62:75–92.
- Yang F, Liu M, Qin N et al. Lipidomics coupled with pathway analysis characterizes serum metabolic changes in response to potassium oxonate induced hyperuricemic rats. *Lipids Health Dis* 2019;18:112.
- Wu X, Zhu JC, Zhang Y et al. Lipidomics study of plasma phospholipid metabolism in early type 2 diabetes rats with ancient prescription Huang-Qi-San intervention by UPLC/Q-TOF-MS and correlation coefficient. *Chem Biol Interact* 2016;256:71–84.
- Sun R, Xu K, Ji S et al. Benzene exposure induces gut microbiota dysbiosis and metabolic disorder in mice. *Sci Total Environ* 2020;705:135879.
- Sun R, Zhang J, Xiong M et al. Altered expression of genes in signaling pathways regulating proliferation of hematopoietic stem and progenitor cells in mice with subchronic benzene exposure. *Int J Environ Res Public Health* 2015;12:9298–313.
- Sun R, Xu K, Ji S et al. Toxicity in hematopoietic stem cells from bone marrow and peripheral blood in mice after benzene exposure: Single-cell transcriptome sequencing analysis. *Ecotoxicol Environ Saf* 2021;207:111490.
- Yang A, Pantoom S, Wu YW. Distinct mechanisms for processing autophagy protein LC3-PE by RavZ and ATG4B. *Chem-biochem* 2020;21:3377–82.
- Patwardhan GA, Beverly LJ, Siskind LJ. Sphingolipids and mitochondrial apoptosis. *J Bioenerg Biomembr* 2016;48:153–68.
- Bai Y, Zhang H, Sun X et al. Biomarker identification and pathway analysis by serum metabolomics of childhood acute lymphoblastic leukemia. *Clin Chim Acta* 2014;436:207–16.
- Marien E, Meister M, Muley T et al. Non-small cell lung cancer is characterized by dramatic changes in phospholipid profiles. *Int J Cancer* 2015;137:1539–48.
- Chu Z, Abu-Baker S, Palascak MB et al. Targeting and cytotoxicity of SapC-DOPS nanovesicles in pancreatic cancer. *PLoS One* 2013;8:e75507.
- Zhao S, Chu Z, Blanco VM et al. SapC-DOPS nanovesicles as targeted therapy for lung cancer. *Mol Cancer Ther* 2015;14:491–8.
- Cui Z, Houweling M, Chen MH et al. A genetic defect in phosphatidylcholine biosynthesis triggers apoptosis in Chinese hamster ovary cells. *J Biol Chem* 1996;271:14668–71.
- Patel D, Witt SN. Ethanolamine and phosphatidylethanolamine: partners in health and disease. *Oxid Med Cell Longev* 2017;2017:4829180.
- Rockenfeller P, Koska M, Pietrocola F et al. Phosphatidylethanolamine positively regulates autophagy and longevity. *Cell Death Differ* 2015;22:499–508.
- Runwal G, Stamatakou E, Siddiqi FH et al. LC3-positive structures are prominent in autophagy-deficient cells. *Sci Rep* 2019;9:10147.
- Qian S, Han Y, Shi Y et al. Benzene induces haematotoxicity by promoting deacetylation and autophagy. *J Cell Mol Med* 2019;23:1022–33.

30. Hanada T, Noda NN, Satomi Y et al. The Atg12-Atg5 conjugate has a novel E3-like activity for protein lipidation in autophagy. *J Biol Chem* 2007;**282**:37298–302.
31. Xie SZ, Garcia-Prat L, Voisin V et al. Sphingolipid modulation activates proteostasis programs to govern human hematopoietic stem cell self-renewal. *Cell Stem Cell* 2019;**25**:639, e637–53.
32. Dewi R, Hamid ZA, Rajab NF et al. Genetic, epigenetic, and lineage-directed mechanisms in benzene-induced malignancies and hematotoxicity targeting hematopoietic stem cells niche. *Hum Exp Toxicol* 2020;**39**:577–95.
33. Morgan GJ, Alvares CL. Benzene and the hemopoietic stem cell. *Chem Biol Interact* 2005;**153–154**:217–22.
34. Wegner MS, Schomel N, Gruber L et al. UDP-glucose ceramide glucosyltransferase activates AKT, promoted proliferation, and doxorubicin resistance in breast cancer cells. *Cell Mol Life Sci* 2018;**75**:3393–410.
35. Ishibashi Y, Ito M, Hirabayashi Y. The sirtuin inhibitor cambinol reduces intracellular glucosylceramide with ceramide accumulation by inhibiting glucosylceramide synthase. *Biosci Biotechnol Biochem* 2020;**84**:2264–72.
36. Li JF, Zheng SJ, Wang LL et al. Glucosylceramide synthase regulates the proliferation and apoptosis of liver cells in vitro by Bcl2/Bax pathway. *Mol Med Rep* 2017;**16**:7355–60.
37. Chen Y, Sun P, Guo X et al. MiR-34a, a promising novel biomarker for benzene toxicity, is involved in cell apoptosis triggered by 1,4-benzoquinone through targeting Bcl-2. *Environ Pollut* 2017;**221**:256–65.
38. Chen Y, Zhang W, Guo X et al. The crosstalk between autophagy and apoptosis was mediated by phosphorylation of Bcl-2 and beclin1 in benzene-induced hematotoxicity. *Cell Death Dis* 2019;**10**:772.
39. Han SH, Kim J, Her Y et al. Phytosphingosine promotes megakaryocytic differentiation of myeloid leukemia cells. *BMB Rep* 2015;**48**:691–5.
40. Nagahara Y, Shinomiya T, Kuroda S et al. Phytosphingosine induced mitochondria-involved apoptosis. *Cancer Sci* 2005;**96**:83–92.
41. Sun R, Cao M, Zhang J et al. Benzene exposure alters expression of enzymes involved in fatty acid beta-oxidation in male C3H/He mice. *Int J Environ Res Public Health* 2016;**13**:1068.
42. Sun R, Meng X, Pu Y et al. Overexpression of HIF-1a could partially protect K562 cells from 1,4-benzoquinone induced toxicity by inhibiting ROS, apoptosis and enhancing glycolysis. *Toxicol In Vitro* 2019;**55**:18–23.
43. Pu Y, Sun F, Sun R et al. PTP4A3, a novel target gene of HIF-1alpha, participates in benzene-induced cell proliferation inhibition and apoptosis through PI3K/AKT pathway. *Int J Environ Res Public Health* 2020;**17**:910.
44. Sun R, Zhang J, Wei H et al. Acetyl-l-carnitine partially prevents benzene-induced hematotoxicity and oxidative stress in C3H/He mice. *Environ Toxicol Pharmacol* 2017;**51**:108–13.
45. Wei H, Zhang J, Tan K et al. Benzene-induced aberrant miRNA expression profile in hematopoietic progenitor cells in C57BL/6 mice. *Int J Mol Sci* 2015;**16**:27058–71.